Annual Report for Period 8/1/03 to 7/31/04

To

The United States Department of Energy
National Energy Technology Laboratory
c/o Contract Specialist: Richard Dunst

Embedded Optical Sensors for Thermal Barrier Coatings

Award DE-FG26-03NT41794

David R. Clarke
Materials Department, College of Engineering
University of California, Santa Barbara

SUMMARY

In this first year of the program we have focused on the selection of rare-earth dopants for luminescent sensing in thermal barrier coating materials, the effect of dopant concentration on several of the luminescence characteristics and initial fabrication of one type of embedded sensor, the "red-line" sensor.

We have initially focused on erbium as the lanthanide dopant for luminescence doping of yttria-stabilized zirconia and europium as the lanthanide for luminescence doping of gadolinium zirconate. The latter exhibits a temperature-dependent luminescence lifetime up to at least 1100^{o}C. A buried layer, "red-line" sensor in an electron-beam deposited yttria-stabilized zirconia coating with erbium has been demonstrated and exhibits a temperature-dependent luminescence lifetime up to at least 400^{o}C.

TABLE OF CONTENTS

1. INTRODUCTION

The primary objective of the first year of this grant has been to identify candidate rare-earth ions that can be incorporated into the crystal structures of the two principal classes to thermal barrier coating materials, yttria-stabilized zirconia (YSZ) and gadolinium zirconate (GZO), and investigate the luminescence properties. To complement these studies and to gain some experience in fabricating sensor configurations, we have experimented in producing a thin, lanthanide-doped layer underneath an otherwise identical thermal barrier coating.

The majority of lanthanide ions are known to give luminescence in the visible range of the optical spectrum and the frequencies of the luminescence lines from the different lanthanides has been well documented. One method of visualizing this knowledge is through the use of the so-called Dieke diagram in which the allowed optical transitions are plotted as energies for different ions. An example is shown in figure 1 for several of the rare-earth ions we have been investigating.

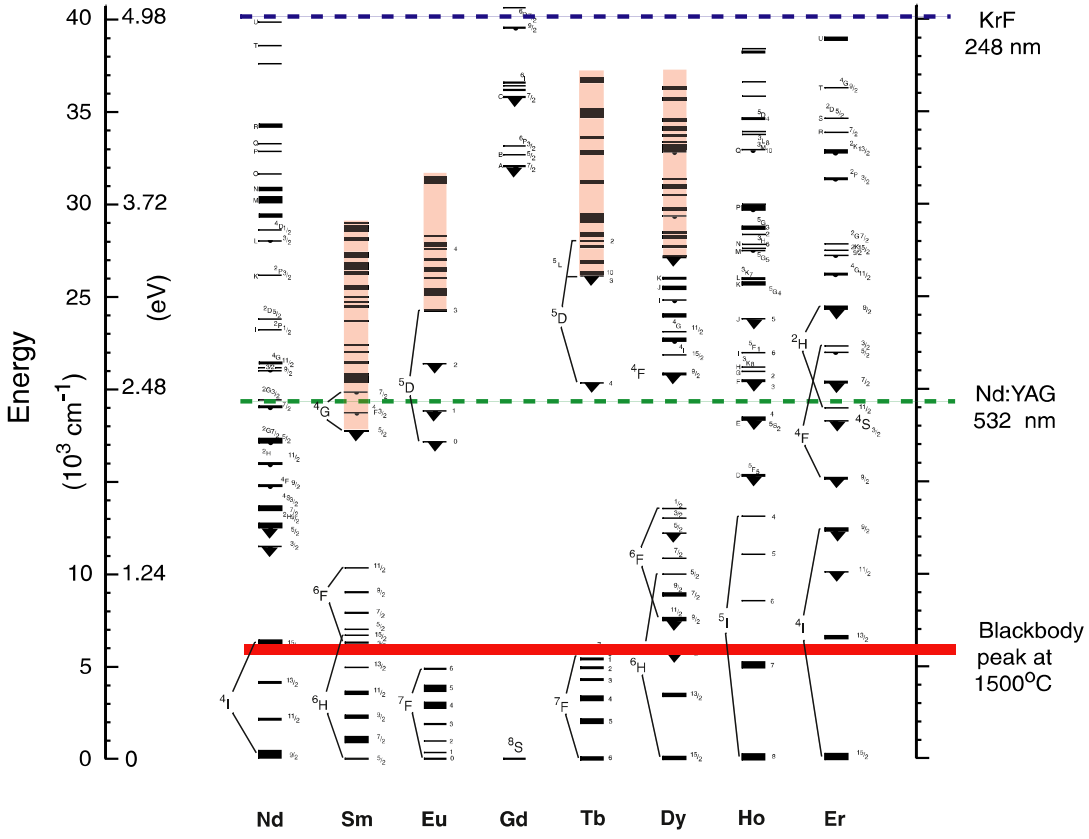

Figure 1. The Dieke diagram for several of the rare-earth ions we have been investigating as candidate dopants for producing sensors in thermal barrier coatings. Also, for reference, are indicated the energies of two of the lasers we employ as well as the energy of the peak in the black-body radiation.

Based on the similarity of ionic size, all the rare-earth ions, ranging from Ce to Yb, in the periodic table are soluble in the crystal structure of both YSZ and GZO and hence are candidate dopants for coatings. Preliminary experiments suggest that of these rare-earth ions, Sm^{3+}, Eu^{3+} and Er^{3+}, all exhibit especially strong luminescence when incorporated into YSZ and GZO materials. Also, comparison with the black-body radiative emission curves also indicate that these ions luminescence at wavelengths below the radiative threshold. Emission from Dy^{3+} also lies below the "black-body" radiation threshold but our preliminary experiments indicate that the luminescence is much weaker than that from the Sm^{3+} and Er^{3+}. For these reasons, our work has concentrated on investigating Sm^{3+}, Eu^{3+} and Er^{3+} dopants.

2. EXPERIMENTAL DETAILS

In seeking to identify appropriate lanthanide dopants and the effect of concentration on luminescence properties, powders and ceramic pellets were synthesized as described in the following sub-section. The two sub-sections following that describe the fabrication of our initial sensor experiments and the characterization of the luminescence properties.

2.1. Synthesis Route

To insure a high degree of uniformity the cation dopant distribution, the lanthanide-doped samples are prepared by a co-precipitation technique for precursor formation, followed by pyrolysis. In this process, solutions of yttrium nitrate ($Y(NO_3)_3.H_20$) and the relevant lanthanide nitrate($M(NO_3)_3*H_20$, where M is the lanthanide) dissolved in DI water are mixed with Zr acetate in the correct proportions to produce the desired molecular percentages of each cation. The number of moles of cation contained in each unit weight of solution was calibrated on the basis of independent calcinations of each solution and a measurement of the resulting mass of oxide (ZrO_2, Gd_2O_3, Y_2O_3, or M_2O_3) product.

The mixed cation solution is gradually introduced (via titration) into NH_4OH (ammonium hydroxide), at a pH of 10-13, to form a (Zr,Y,M)OH reaction product, which is obtained from the mixture by vacuum filtering. The remaining water that adsorbed, physically and chemically, onto the mixed hydroxide, is driven off by heating at ~150^{o}C. A calcination step is then performed in air at 950^{o}C to remove hydroxide groups and form the oxide. Finally, the formation of the YSZ t' phase, with a complete mixing of the cations on the crystal lattice, is insured by sintering at 1200^{o}C for two hours.

2.2. Sensor Fabrication

Initial sensor configurations have been fabricated by electron-beam evaporation (EB-PVD) from zirconia ingots. The initial configuration we have studied is shown in figure 2. We have chosen EB-PVD for these initial explorations since it requires less lanthanide-doped material than plasma-spraying.

The electron-beam depositions were performed at UCSB using our dedicated electron-beam evaporation system. We developed an innovative

method of incorporating the lanthanide into the standard, commercial 7YSZ ingots for evaporation. The method consists of three steps. The first is infiltrating the ingots, which are porous, with nitrate solutions of the lanthanide. The second is an intermediate temperatures, typically 200-300°C, to convert the nitrate into a mixed hydroxide. This infiltration/drying process is repeated until the desired lanthanide concentration is reached. Then, in the third step, the infiltrated ingot is heated in air at 950°C to remove hydroxide groups and form the lanthanide oxide throughout the ingot.

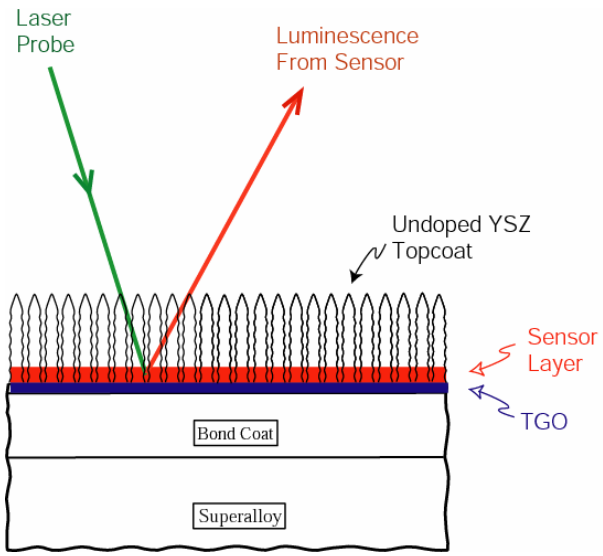

Figure 2. Schematic diagram illustrating the embedded "red-line" sensor configuration that has been the focus of our initial attempts to fabricate viable luminescence sensors.

2.3. Luminescence Characterization

The luminescence properties of the lanthanide-doped materials and initial sensors were characterized by two principal methods. One was the spectral characterization using a laser-based photo-stimulated luminescence system in which the luminescence excited by the laser was collected with a fiber-optic and analyzed with an optical spectrometer. The other was the measurement of the luminescence lifetime. These measurements were made with a pulse laser, a diffraction grating and a photomultiplier detector all, under control of a computer. The laser pulse was triggered and the excited luminescence collected with a fiber optic, passed through the grating to select the luminescence line of interest and into the photomultiplier. The output was recorded as a function of time and the lifetime determined from a semi-logarithmic plot of intensity vs. time. For the temperature dependent measurements, the sample was positioned in a furnace and the luminescence collected with a high-temperature optical fiber positioned within the furnace.

3. RESULTS

As mentioned above, based on preliminary measurements, our work in the first year has concentrated on investigating Sm^{3+} , Eu^{3+} and Er^{3+} dopants, specifically, Sm^{3+} and Er^{3+} dopants in YSZ and Eu^{3+} dopant in GZO materials.

3.1. Concentration Effects on the Luminescence Spectra

Based on prior knowledge in the luminescence literature, the photoluminescence intensity and lifetime of the luminescence from rare-earth dopants in thermal barrier materials can be expected to be dependent on dopant concentration. To investigate, the effect of dopant concentration, we produced a series of compositions represented as:

$$Zr^{4+}_{1-x-y}Y^{3+}_{x}RE^{3+}_{y}O^{2-}_{2-x-y}D_{x+y} \quad \text{and} \quad Gd_{2(1-x)}RE_{2x}Zr_2O_7$$

where *RE* represents the rare-earth dopant and *D* represents the structural vacancies introduced by the dopants. In the case of the YSZ materials, we have held the Y^{3+} concentration constant, x, at 0.07, which without the rare-earth corresponds to the commercial YSZ coating material.

Examples of the effect of varying the dopant ion concentrations are shown in figures 3 and 4 for Er^{3+} and Eu^{3+} dopants.

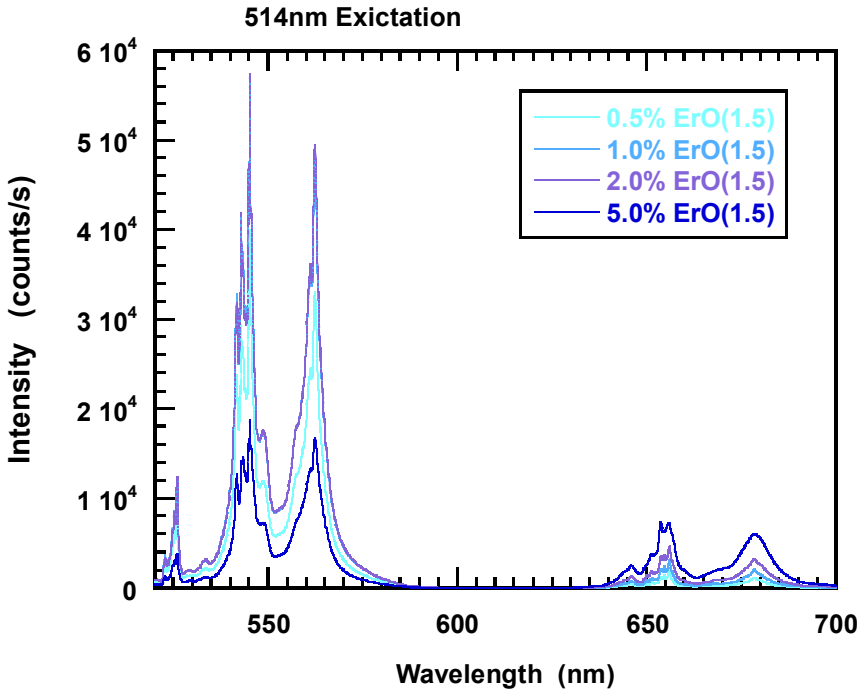

Figure 3. Effect of concentration of $ErO_{1.5}$ in YSZ on the luminescence excited with a laser at 514 nm.

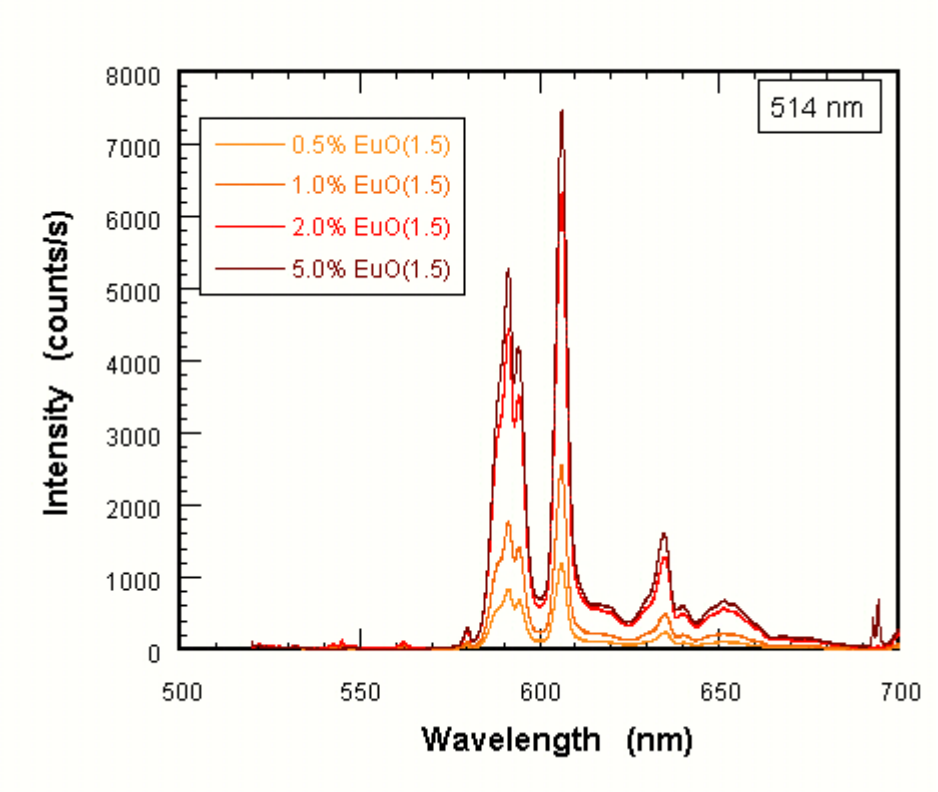

Figure 4. Variation in the luminescence spectrum with concentration of $EuO_{1.5}$. The luminescence was excited with an argon-ion laser at 514 nm.

Examination of the spectra reveals that the effect of dopant concentration varies from one spectral line to another. An example of this variation is shown for four different spectral lines in figure 5, for Er^{3+} doped YSZ. Interestingly, two distinct behaviors are observed. For the lines at 543 nm and 562 nm, the concentration dependence is similar to standard phosphors, showing three distinct regimes. At low concentrations, the luminescence intensity varies linearly with concentration as is expected for isolated ions. It then becomes sub-linear as the ions begin to interact and the intensity peaks. At still higher concentrations, the intensity decreases with increasing concentration. This behavior is illustrative of concentration quenching. The variation of the intensity of the lines at 654 and 678 nm is quite different, exhibiting a linear increase with concentration. The reasons for the linear variation and why the behavior of the different lines is so different have yet to be fully understood. Nevertheless, the differences have important consequences for fabricating viable sensors since some compositional variation is inevitable in any TBC deposition process. If tight compositional control cannot be maintained, then the data in figure 5 suggests that sensing with the longer wavelengths might be preferably despite the lower luminescence intensity. This is especially so if the relative strength of luminescence lines are to be used as a method of temperature measurement. (This is not our approach but has been suggested by others).

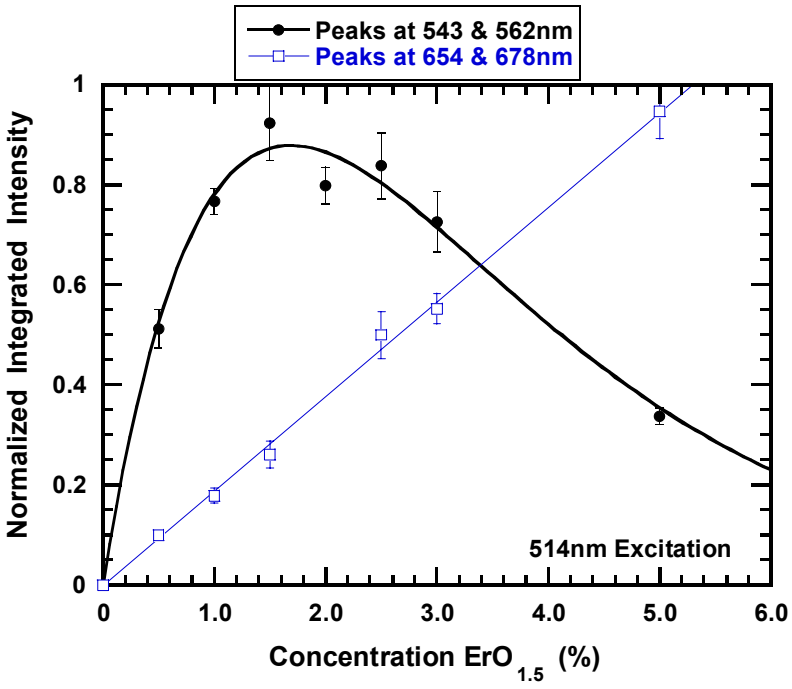

Figure 5. Variation in luminescence intensity for different spectral lines shown in figure 3 as a function of $ErO_{1.5}$ concentration in YSZ materials. The data is normalized to the maximum intensity of the 543 nm line.

Similar behavior has been observed for both Sm^{3+} and Eu^{3+} doping as a function of concentration. A fuller description of all the data will be given in a manuscript being prepared for publication.

3.2. Temperature Dependence of Luminescence of Eu^{3+} doped GZO

Experiments have been carried out to investigate the temperature dependence of the luminescence from GZO materials doped with Eu^{3+} ions. The material investigated was in the form of a ceramic pellet synthesized as described in section 2.1 and then sintered to 1500°C in air. The measurements were made from room temperature up to 1100°C, the maximum temperature we can reach with our present furnace capabilities.

At all temperatures, the luminescence intensity decayed with a double exponential dependence on time. The data shown in figure 6 is of the longer decay time and much of the scatter shown in the figure is due to difficulties in accurately determining the lifetime. This is an important issue so we will be developing a more refined method for extracting the pertinent lifetimes from such double-exponentials in future.

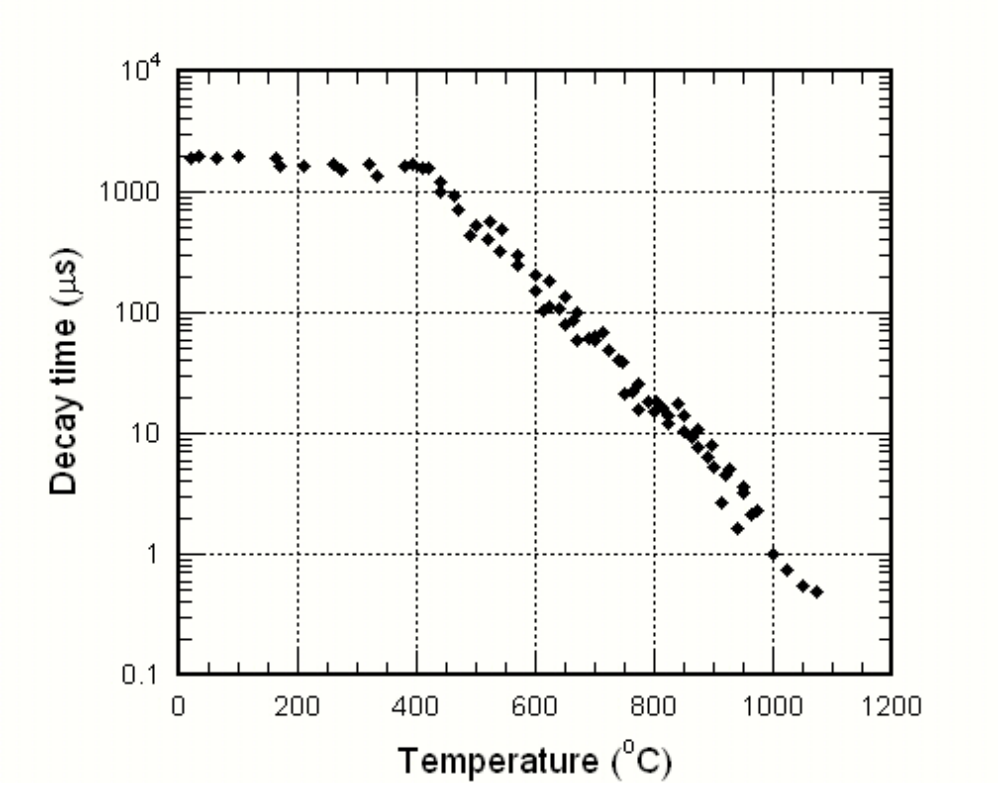

Figure 6. The observed temperature dependence of the 610 nm luminescence line of Eu-doped GZO. The excitation was with a 248 nm excimer laser. Sample composition $Gd_{1.98}RE_{0.02}Zr_2O_7$. *Curves such as these provide the calibration required to use luminescence decay times for measuring temperature.*

3.3. "Red-Line" Sensor using Er^{3+} doping of YSZ

The concept of the "red-line" sensor is that it is a dual-purpose sensor. One application is for the measurement of temperature in the TBC adjacent to the alloy component. The other is as an indication of when the coating has worn or eroded away leaving only a thin, remnant layer on the surface of the alloy component. The former requires that the doped sensor layer has a temperature dependent luminescence. The later requires that its luminescence only becomes visible when the sensor layer is exposed.

Both of these potential applications require that the sensor layer is buried underneath an undoped layer. The former also requires that the dopant layer can be excited with a suitable laser wavelength and the luminescence collected through the outer layer. The latter requires the choice of a laser wavelength that does not penetrate through the un-doped coating so that it is only when the un-doped portion of the coating has been removed that the luminescence from the "red-line" layer is collectable.

To gain some practical experience in making such sensors, we have deposited the configuration shown in figure 2 with the sensor layer made of Er-doped YSZ with an outer layer of 120 micron thick undoped, commercial YSZ coating. Figure 7 presents the luminescence spectra from the buried sensor using

two different laser wavelengths. One, at 514 nm, penetrates through the undoped YSZ and the other, at 248 nm, is heavily absorbed in the undoped YSZ. As the spectra in figure 7 indicates, the characteristic luminescence lines from the buried Er-doped YSZ layer can be detected when the 514 nm laser is used whereas there is no luminescence from the buried layer when the same sensor sample is interrogated with the 248 nm laser. Additional confirmation that the 514 nm can penetrate through the coating comes from the appearance of the strong doublet at ~ 695 nm which is the characteristic luminescence from Cr^{3+} ions incorporated into the thermally grown oxide during high temperature oxidation.

For the example shown in figure 7, a laser with a wavelength similar to many solid-state lasers was chosen but other lasers in the visible were also used demonstrating that a range of wavelengths can be used to probe the buried layer sensor. For instance, the same spectra was obtained using a pulsed laser operating at 355 nm.

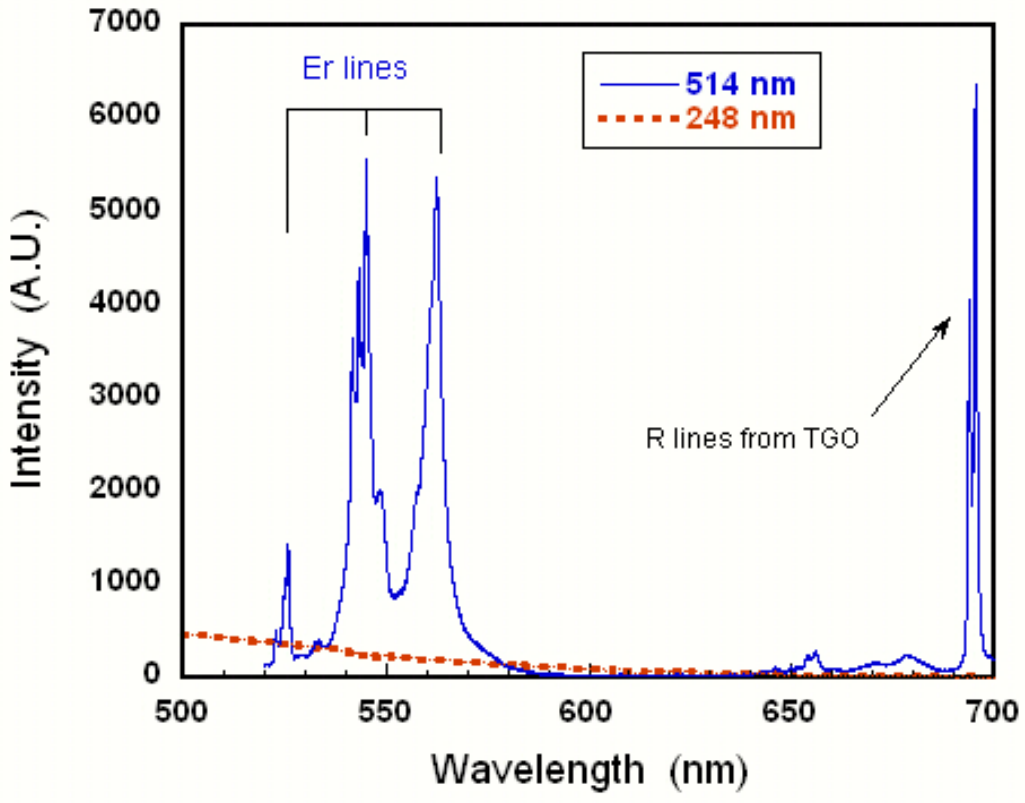

Figure 7. A comparison of the luminescence spectra from a zirconia TBC sample with a buried, 10 micron thick Er-doped zirconia layer in contact with the bond-coated superalloy and covered with ~ 120 microns of standard, undoped YSZ coating. The comparison shows that the buried sensor layer can be probed using a laser in the visible but cannot be probed in the UV where the undoped zirconia heavily absorbs.

Initial results have also been obtained of the temperature dependence of the buried layer luminescence. (Figure 8). The luminescence lifetime of the Er-doped YSZ is considerably shorter than that of Eu-doped GZO shown in figure 6 but is detectable nonetheless, at least up to 400°C. Modifications of the detector circuits are underway to enable us to detect even shorter lifetimes. These will determine to what temperature Er-doping of YSZ may be a viable TBC sensor.

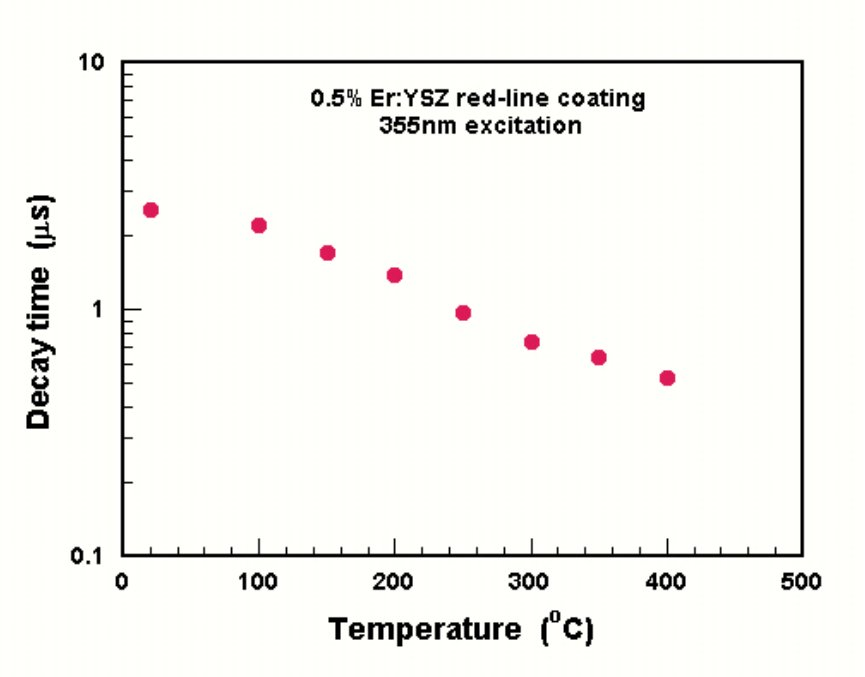

Figure 8. Variation in temperature of the luminescence decay time from the buried Er-doped YSZ sensor layer.

4. CONCLUSION

We have demonstrated in the first year of this program several results that are relevant to the development of luminescence sensors for *in-situ* sensing of thermal barrier coatings in gas turbines. The first is that several rare-earth ions can be incorporated into the crystal structure of two of the commonest thermal barrier coating materials, yttria-stabilized zirconia and gadolinium zirconate, and produce strong luminescence. The second is that the effect of concentration on the intensity of luminescence has been measured, which points the way to the selection of optimum rare-earth doping for sensors. The third important result is that the luminescence from Eu^{3+} doping in gadolinium zirconate exhibits a measurable variation in luminescence lifetime from 400°C to at least 1100 °C. This suggests that coating temperatures in this range can, in principle, be measured by luminescence for a real coating. The fourth result is that a buried layer sensor, consisting of an inner layer containing the sensor underneath an undoped YSZ coating, can be fabricated by a standard commercial deposition process and that its luminescence is readily probed and not degraded by the deposition process.